International Research Journal of Engineering and Technology (IRJET) e-ISSN: 2395-0056
Volume: 06 Issue: 08 | Aug 2019 www.irjet.net p-ISSN: 2395-0072

Modelling and Optimization of Heat Transfer Coefficients for Hot and Cold Sides of Thermoelectric Generator (TEG) system

R. Elankovan[1], S. Suresh[2], K Karthick[3]

[123] *Department of Mechanical Engineering, National Institute of Technology, Tiruchirappalli, Tamil Nadu, India.*

Abstract – *The race for exploring alternative energy source to replace the dependency of fossil fuels based energy is gaining significant attention due to the rise of global warming and other emission issues. Thermoelectric generator (TEG) is emerging as a promising member in alternative energy sources to restrict the consumption of fossil fuel for some extent. The advent of TEG to recover waste heat is a momentous in industrial applications. However, the thermal system of TEG for heat recovery applications need to be optimized to make it a viable option. This paper presents the impact of heat transfer coefficients (HTC) on the performance of TEG through simulation works carried out in ANSYS 17®. The impact of HTC on the hot side and cold side temperature of TEG couple is studied by varying heat source and heat sink temperatures for optimizing the performance of TEG. The results presented shows that the voltage and temperature difference will be higher with increase in cold side HTC rather than increasing hot side HTC. The percentage difference in voltage as well as for temperature is same for a set of hot side and cold side heat transfer coefficient. The maximum power output is generated for each heat transfer coefficient at a matched load resistivity of 0.00015 Ωm. In this study, the power output reaches saturation with increase in hot side heat transfer coefficient while the cold side heat transfer coefficient is approximately 50 times higher than that of hot side heat transfer coefficient. The drop in the voltage and difference in temperature also increases with increase in heat source temperature and heat sink temperature.*

Keywords: Thermal System Configuration, Heat Transfer Coefficient, Heat Source and Sink Temperature and Thermo electric generator (TEG)

1.INTRODUCTION

The requisite for development of alternative energy sources to reduce the fossil fuel consumption has attained topmost priority to reduce the impact of emission of fossil fuel. The sole dependency of fossil fuel for power generation over the years has resulted in global warming, ozone depletion and other environmental degradation issues. The above said problem is the challenge for which there is an exorbitant rise of research interest is seen in the field of renewable energy over the last few years. At this context TEG acts as a promising member in the field of energy recovery. Although TEGs performance is greatly restricted due to less conversion efficiency, TEG continues to dominate in the field of waste heat recovery. Research suggests that 60% of the total energy is wasted in the form of heat which is in the form of low grade heat energy [1]. The application of TEG in converting waste heat into power output has gained attention all over the world and the research interest in this field has increased significantly over the last three decades. A thermoelectric generator (TEG) is a solid-state device, which can directly convert heat into electricity which is based on the discovery of Seebeck effect by which temperature difference is directly converted into heat. The heat to electricity conversion has an efficiency of less than 5% [2-3]. Therefore, the concern on improving the conversion efficiency of TEG is vital to use it as a viable tool to recover waste heat. The dominance of TEG on par with other sources of energy lies in the utilization of costless waste heat as energy input which makes it suitable for applications which are not affected by its low conversion efficiency [4]. The various applications of TEG range from recovering waste heat from fossil fuel fired boilers, automobile exhaust [5-9] to industrial operations such as biomass boiler [10], small scale pellet boiler [11], cement plants, marine waste incinerator [12], refineries, glass manufacturing, and foundries. Other areas of implementation include wood burning stoves [13], geothermal sites, solar salt ponds and solar concentrators [14].

The ill effects of fossil fuel burning can be mitigated and minimized to an extent by the effective introduction of the thermoelectric generators. The reliability of the thermoelectric effect in the electrification of waste heat has been validated by experiments conducted for different industrial process. The literature in the past indicates that the power output from TEG is directly proportional to the temperature difference between the hot and cold faces of the TEG. In a TEG thermal configuration system, the hot and cold face temperatures depend on the heat transfer coefficients on the respective sides. This paper emphasis the impact of variation in heat transfer coefficients on hot and cold sides of TEG through simulation using ANSYS 17® multi-physics software.

2. COMPUTATIONAL MODELLING AND BOUNDARY CONDITIONS

2.1. TEG model

The thermoelectric generator module contains of p and n type semiconducting materials which are connected electrically in series and thermally in parallel. In this case a pair of thermocouple is considered for simulation. A single p and n junction pair of a TEG with 97 couples is analysed. The Thermo-electric Multi-physics simulation is modelled and simulated in 3D using ANSYS 17®. The material properties of the TEG Couple is given in Table 1.

Table 1: Material Properties of the TEG couple

S No	Description	Value
1	Thermal conductivity of top and bottom copper bar	401 W/m°C
2	Resistivity of top and bottom copper bar	2.27X10-8 Ωm
3	Thermal conductivity of P-Junction	2.3 W/m°C
4	Resistivity of P-Junction	1.64X10-5 Ωm
5	Seebeck Coefficient of P-Junction	0.00022 V/°C
6	Thermal conductivity of N-Junction	2.3 W/m°C
7	Resistivity of N-Junction	1.64X10-5 Ωm
8	Seebeck Coefficient of N-Junction	-0.00022 V/°C

2.2. Governing equation

Accounting the coupling mechanisms of Seebeck, Peltier and Thomson effects on TEG system between electrical and thermal fields, a fully coupled field model is developed by generating governing equations under steady-state conditions for both electrical potential profiles and temperature in the absence of input magnetic field [26].
By taking Joule heating into account in the process, the equation for energy conservation is given by

$$\nabla\,(k\,.\nabla T) - T\,.J\,.\frac{\partial \alpha}{\partial T} + \rho_{teg}\,.J = 0 \quad (9)$$

Now, applying thermoelectric effect into coupling of heat flow equation and electric charge continuity equation,

$$\nabla\,.J = 0 \quad (10)$$

Where J is the electric current density vector.
Above two equations are coupled by the set of thermoelectric constitutive equations

$$q = [\Pi].J - [k]\,.\nabla T \quad (11)$$

$$J = [\sigma_e]\,.(E - [\alpha].\nabla T) \quad (12)$$

Where,
[σe] = electrical conductivity matrix
[k] = thermal conductivity matrix
[α] = Seebeck coefficient matrix
[Π] = T[α] is the Peltier coefficient matrix

As per model, in the absence of time varying magnetic field, E will become irrotational and derived from an electric scalar potential (ϕ)

$$E = -\nabla\phi \quad (13)$$

Hence, electric power expression is given by

$$P_o = \frac{{V_{oc}}^2}{2(R_{teg} + R_L)} \quad (14)$$

For obtaining maximum electric power, RL = Rteg
The basic set of thermoelectric equations of TEG determines the five state vector parameters Qh, Qc, Th, Tc and Io. Now for any change in operation condition, TEGs will shift to a new stage for balancing the equations. When the state vector stabilizes, power output and conversion efficiency values are obtained. The equations described in the previous section are solved using the ANSYS which is the commercial software based on the finite element method and is applicable to multiphysics problems [13].

2.3. Mesh and the Boundary Conditions

A pair of p and n junction of TEG is employed for simulation. A 3D structured mesh and a fine mesh are applied over the entire area of TEG couple. The 3D mesh in an isometric view of TEG p and n junction is shown in Fig.1 where individual components are labelled and respective dimensions of TEG couple are also mentioned in mm. The boundary conditions for TEG couple is discussed in Table 2.

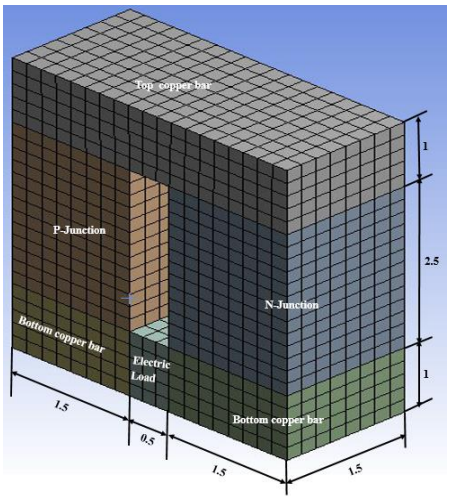

Fig. 1: Mesh of TEG Couple

Table 2: Boundary conditions of the TEG couple

S No	Description	Value
1.	Resistivity of Electric Load (ρ)	1X10-6 to 1X10-3 Ωm
2.	Heat Transfer coefficient of TEG hot side (hhs)	10 to 5000 W/m²C
3.	Heat Transfer coefficient of TEG cold side (hcs)	10 to 5000 W/m²C
4.	Hot source Temperature (Ths)	100 to 200 ˚C
5.	Heat sink Temperature (Tcs)	25 to 50 ˚C
6.	Ground on N-Junction bottom copper bar (Vo)	0 mV

3. SIMULATION RESULTS

3.1 Effect of heat transfer coefficient on hot and cold side of TEG couple for open circuit condition

The effect of heat transfer coefficient on hot and cold side of TEG couple is studied through simulation considering the following input conditions. The heat source temperature is kept constant temperature of 200 °C, with heat sink exposed to ambient temperature of 30 °C for the same 1.5 mm x 1.5 mm square size of the p-type and n-type junction legs of length 2.5 mm. The thermal conductivity of TEG is assumed as 2.3 W/m°C. The influence of hot and cold side heat transfer coefficient on open circuit voltage is studied by constant low cold side heat transfer coefficient of 10, 50, 100, 500, 1000, 5000 W/m²C for different hot side heat transfer coefficient of 10, 50, 100, 500, 1000, 5000 W/m²C. The maximum heat transfer coefficient (5000 W/ W/m²C) is simulated to evaluate the performance at high heat transfer coefficient values, the application of TEG at high heat transfer coefficient accounts for complexity of the thermal configuration system. However, the results were in accordance with practical heat transfer coefficient cases.

The effect of hot side and cold side heat transfer coefficients are observed in TEG couple for open circuit condition. The effect of heat transfer coefficient in hot side and cold side temperature for open circuit simulations is shown in Fig. 2a. The open circuit voltage produced for varying hot side heat transfer coefficients for a low cold side heat transfer coefficient of 10 W/m² °C is shown in Fig. 2b. The open circuit voltage generated for hot side heat transfer coefficients of 10, 50, 100, 500, 1000, 5000 W/m²C is 0.43523, 0.76123, 0.83987, 0.91553, 0.92595, 0.93447 mV respectively for a minimum cold side heat transfer coefficient of 10 W/m²C. Similarly, the open circuit voltage produced for cold side heat transfer coefficients of 10, 50, 100, 500, 1000 W/m²C is 0.8029, 3.8237, 7.2186, 24.916, 35.926 55.569 mV for a minimum of hot side heat transfer coefficient of 10 W/m²C. It can be inferred that the open circuit voltage peaked a value of 55.569 mV for a heat transfer coefficient of 5000 W/m2C at cold side with a minimum heat transfer coefficient at hot side.

Similarly, the voltage rise achieved a maximum value of 0.93447 mV for a heat transfer coefficient of 5000 W/m²C at hot side with a minimum heat transfer

coefficient at cold side. This illustrates that for a given minimum cold side heat transfer coefficient, the increase in voltage and temperature difference is lesser when compared to higher hot side heat transfer coefficients for various cold side heat transfer coefficients. The percentage difference in voltage and temperature difference for set of hot side and cold side heat transfer coefficient is more or less the same. It can be observed that the voltage and temperature difference is higher by increasing cold side heat transfer coefficient. The open circuit temperature contours of TEG couple for typical set hot side and cold side heat transfer coefficients is shown in Fig. 3 and the open circuit voltage contours of TEG couple for typical set hot side and cold side heat transfer coefficients is shown in Fig. 4.

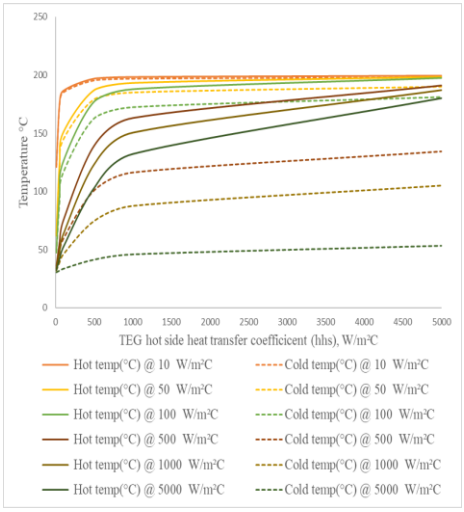

Fig. 2a: Effect of hot side heat transfer coefficients on difference in temperatures between hot and cold sides of TEG for a cold side heat transfer coefficient of 10 W/m² °C in open circuit.

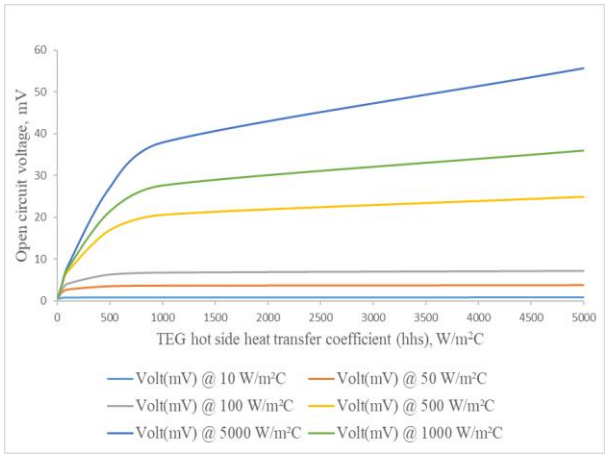

Fig. 2b: Effect of hot side heat transfer coefficients on open circuit voltage for a cold side heat transfer coefficient of 10 W/m² °C

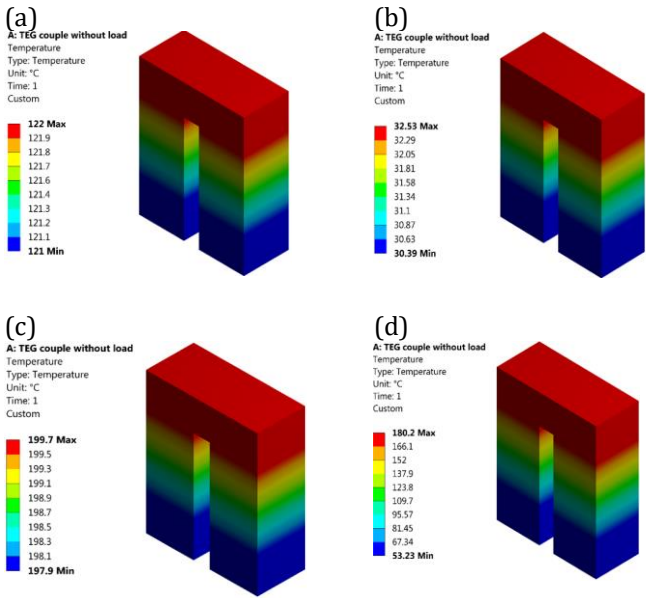

Fig. 3: Temperature Contours of TEG couple with open circuit at (a) hhs-10W/m²C and hcs- 10W/m²C, (b) hhs-10W/m²C and hcs-5000W/m²C, (c) hhs-5000W/m²C and hcs-10W/m²C and (d) hhs-5000W/m²C and hcs-5000W/m²C.

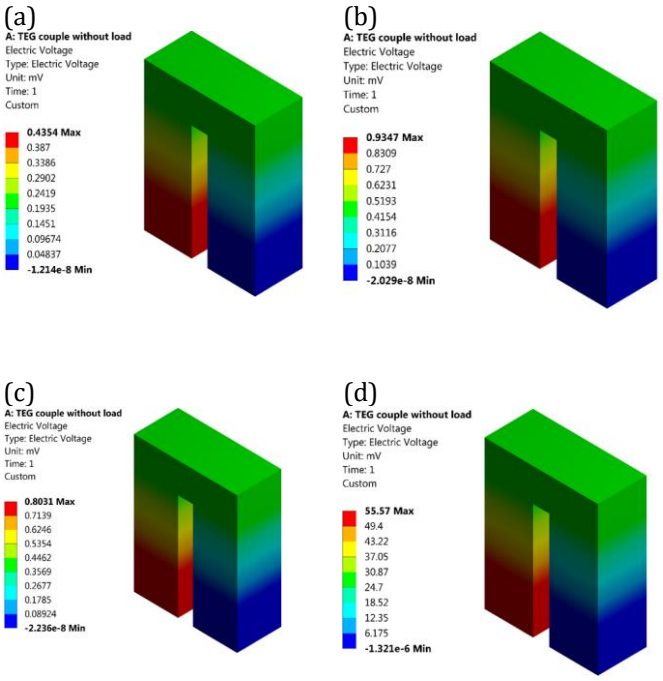

Fig. 4: Open circuit voltage Contours of TEG couple at (a) hhs-10W/m²C and hcs- 10W/m²C, (b) hhs-10W/m²C and hcs-5000W/m²C, (c) hhs-5000W/m²C and hcs-10W/m²C and (d) hhs-5000W/m²C and hcs-5000W/m²C.

3.2 Effect of convective heat transfer coefficients on output power for varying resistivity of TEG couple:

The performance of TEG power output due to the effect of electrical load resistivity for typical set hot side and cold side heat transfer coefficients is shown in Fig. 5 to Fig. 9. The fluctuations that occur during the power generation is due to the Seebeck co-efficient because during the simulation it was assumed to be constant where actually it depends on the temperature. It was observed that the power output of the TEG increases with the increase in heat transfer coefficient between the two sides. The power output of TEG is maximum at the matched load resistivity. From the study, the matched load resistivity is found to be 0.00015 Ωm. Therefore, the maximum power output is generated for each heat transfer coefficient with a highest individual value at matched load resistivity (0.00015 Ωm).

The minimum value of all is 1.07 μW for which the hot side heat transfer coefficient (hhs) is 10 W/m²C and cold side heat transfer coefficient (hcs) is10 W/m²C. Similarly, the maximum value of all is 23395 μW for hhs=5000 W/m²C and hcs=5000 W/m²C.

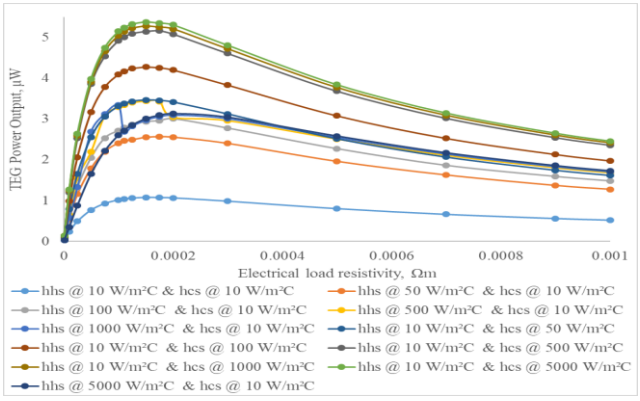

Fig. 5: Behaviour of thermoelectric power for varying heat transfer coefficients of cold/hot side and corresponding hot/cold side at 10 W/m²C

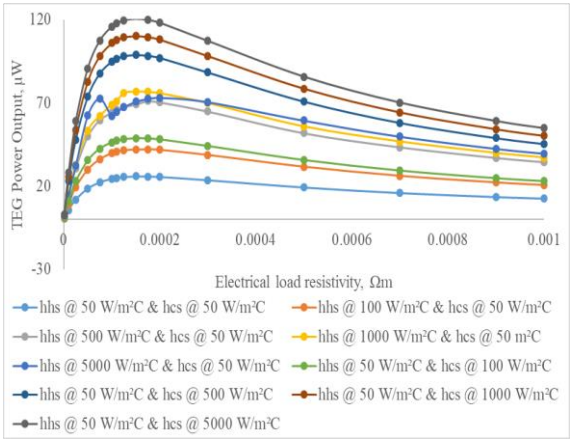

Fig. 6: Behaviour of thermoelectric power for varying heat transfer coefficients of cold/hot side and corresponding hot/cold side at 50 W/m²C

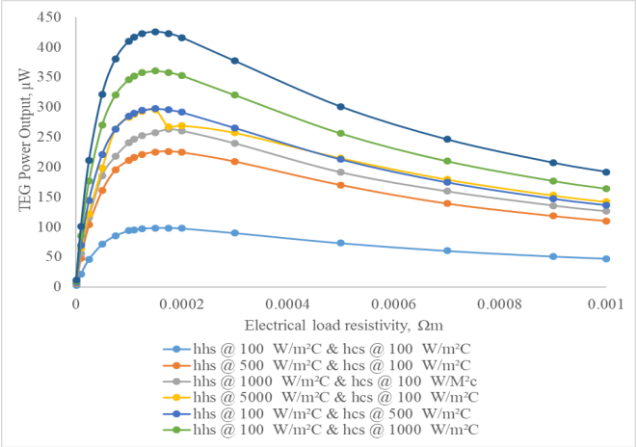

Fig. 7: Behaviour of thermoelectric power for varying heat transfer coefficients of cold/hot side and corresponding hot/cold side at 100 W/m²C

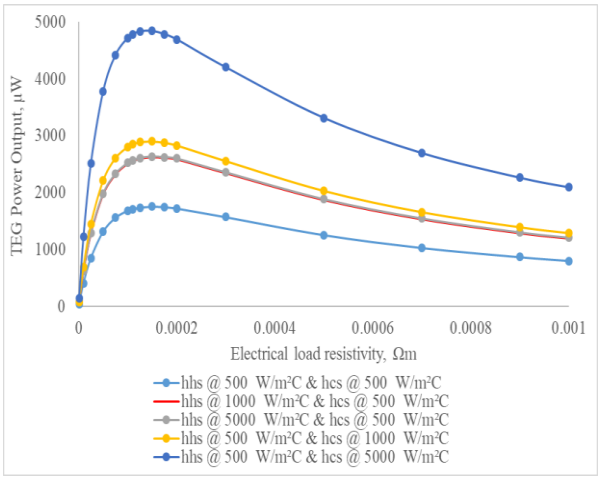

Fig. 8 Behaviour of thermoelectric power for varying heat transfer coefficients of cold/hot side and corresponding hot/cold side at 500 W/m²C

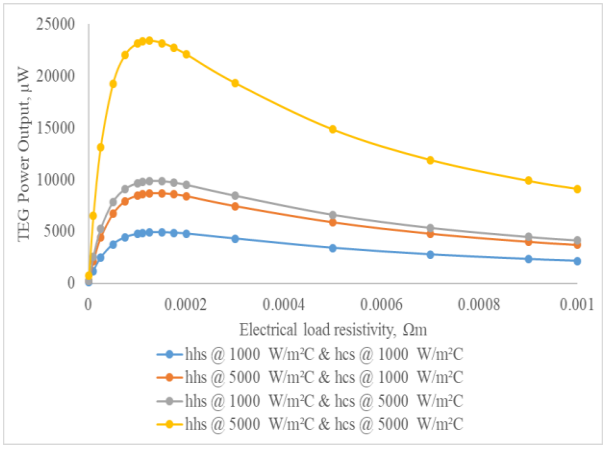

Fig. 9: Behaviour of thermoelectric power for varying heat transfer coefficients of cold/hot side and corresponding hot/cold side at 1000 W/m²C

The TEG power output is plotted for hot side heat transfer coefficient with respect to cold side heat transfer coefficient conditions and for cold side heat transfer coefficient with respect to hot side heat transfer coefficient condition is shown in Fig. 10 to Fig. 14. The graphical abstract follows a common syntax in considering hot side heat transfer coefficient varying in x-axis for solid-line plots and cold side heat transfer coefficient varying in x-axis for dotted-line plots. The results figure out that for the same applied electric load, the increase in power output is more when there is an increase in the heat transfer coefficient on the cold side rather than compared to increase in heat transfer coefficient hot side. It is observed that the TEG power output will not have any significant increase with the increase of heat transfer coefficient after a certain extent. Fig. 10 shows that for all electrical load resistivity the percentage of power output obtained by fixing cold side heat transfer coefficient 10 W/m²C. The hot side heat transfer coefficient 50 W/m²C is 26 % approximately higher than that of fixing hot side heat transfer coefficient 10 W/m²C, cold side heat transfer coefficient 50 W/m²C. The percentage increase of power output obtained by fixing cold side heat transfer coefficient 10 W/m²C, hot side heat transfer coefficient 5000 W/m2C is 44 % approximately higher than that of fixing hot side heat transfer coefficient 10 W/m²C, cold side heat transfer coefficient 5000 W/m²C. While fixing hot side and cold side heat transfer coefficient at 10 W/m²C, the power output obtained by hot side and cold side heat transfer coefficient at 500 W/m²C is approximately 79 % higher and there is no significant improvement in power output for more than 500 W/m²C in this case. Hence, it is significant that the power output reaches saturation in increasing hot side heat transfer coefficient whereas the cold side heat transfer coefficient is approximately 50 times higher than that of hot side heat transfer coefficient. In all the other cases, the power output is influenced by both cold side and hot side heat transfer coefficient follow same trend as before.

The closed circuit temperature contours of TEG couple for typical set hot side and cold side heat transfer coefficients is shown in Fig. 15, also the closed circuit voltage contours of TEG couple for typical set hot side and cold side heat transfer coefficients is shown in Fig. 16. The closed circuit total current density vector of TEG couple for typical set hot side and cold side heat transfer coefficients is shown in Fig. 17.

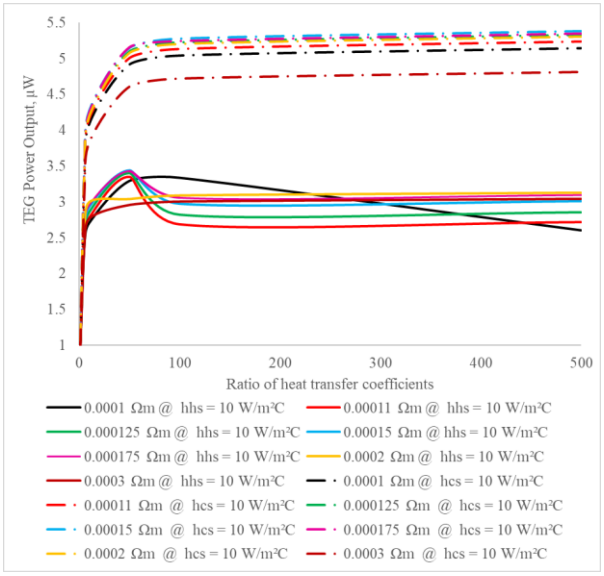

Fig.10: Comparison of effect on TEG power output for varying heat transfer coefficients of cold/hot side and corresponding hot/cold side at 10 W/m²C.

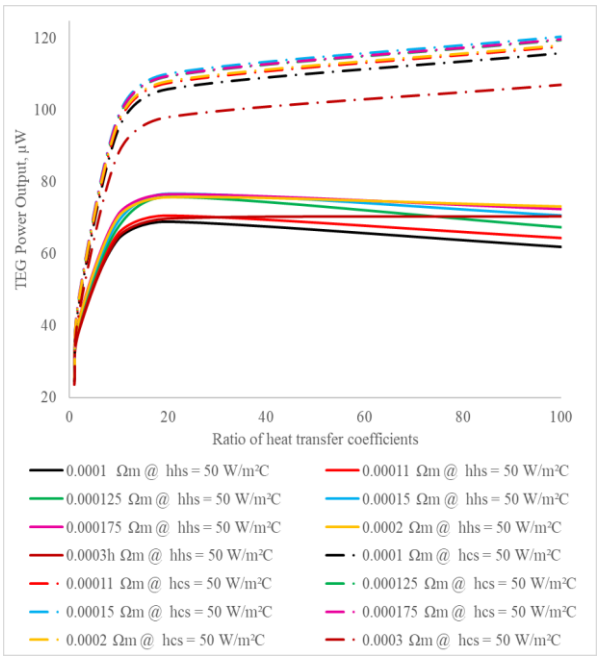

Fig. 11: Comparison of effect on TEG power output for varying heat transfer coefficients of cold/hot side and corresponding hot/cold side at 50 W/m²C.

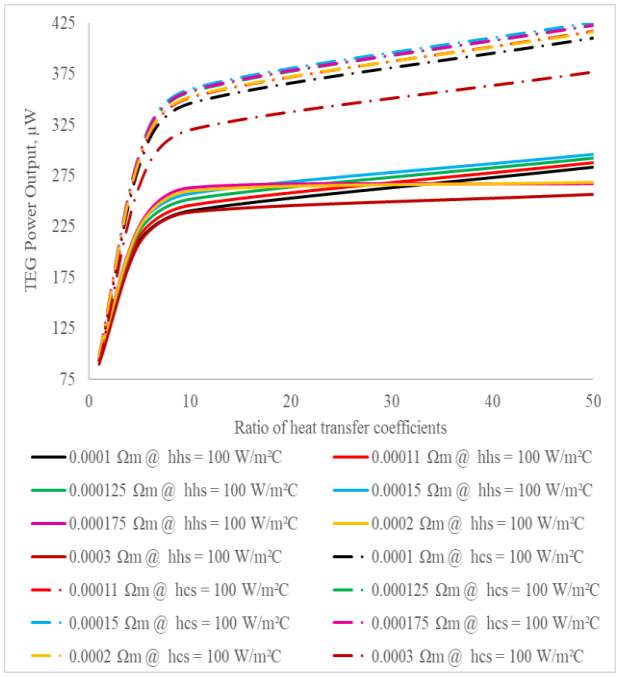

Fig. 12: Comparison of effect on TEG power output for varying heat transfer coefficients of cold/hot side and corresponding hot/cold side at 100 W/m²C.

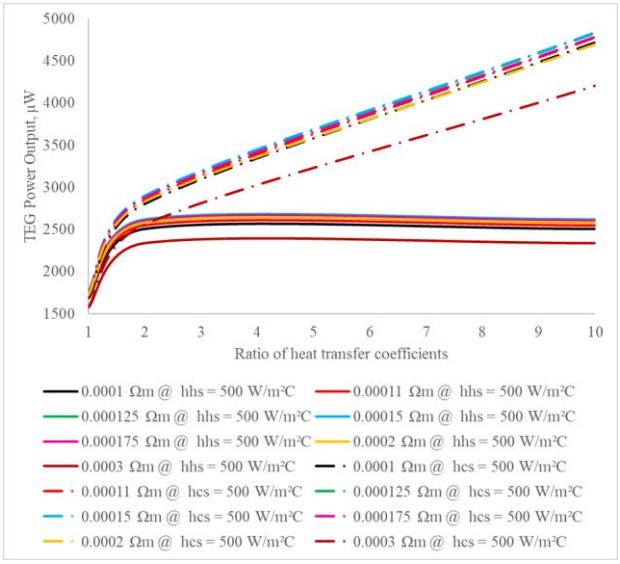

Fig.13: Comparison of effect on TEG power output for varying heat transfer coefficients of cold/hot side and corresponding hot/cold side at 500 W/m²C.

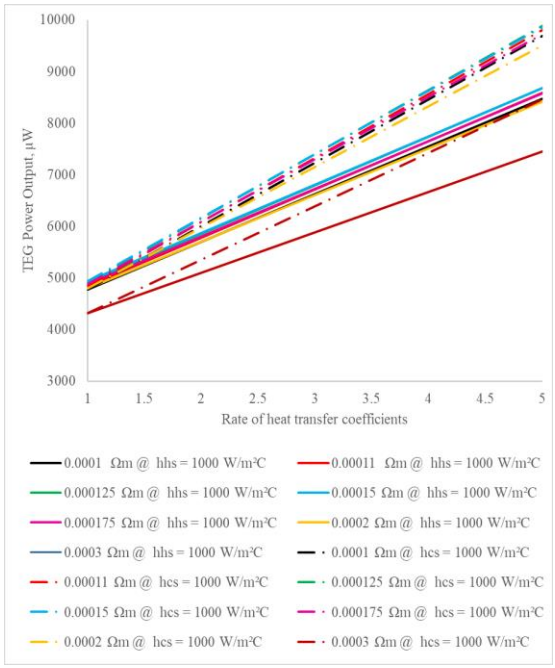

Fig. 14: Comparison of effect on TEG power output for varying heat transfer coefficients of cold/hot side and corresponding hot/cold side at 1000 W/m²C.

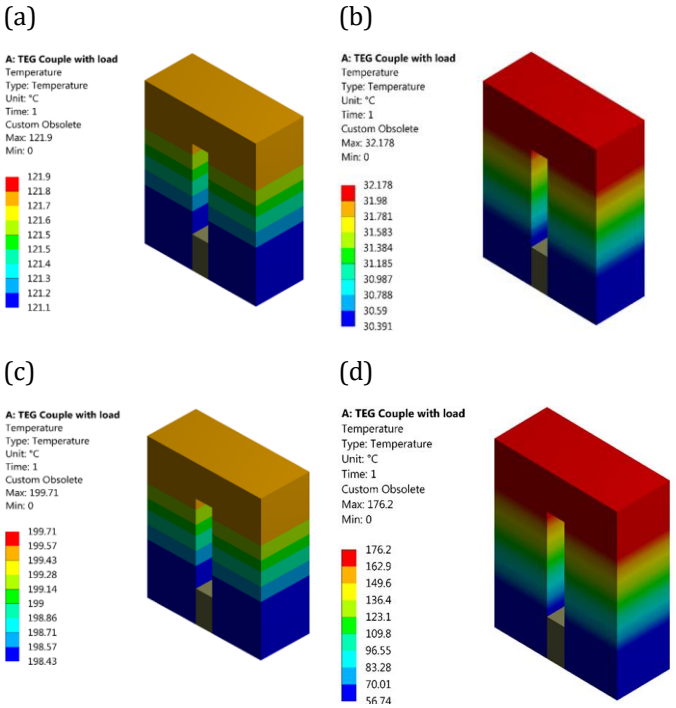

Fig. 15: Temperature Contours of TEG couple with closed circuit at (a) hhs-10W/m²C and hcs- 10W/m²C, (b) hhs-10W/m²C and hcs-5000W/m²C, (c) hhs-5000W/m²C and hcs-10W/m²C and (d) hhs-5000W/m²C and hcs-5000W/m²C.

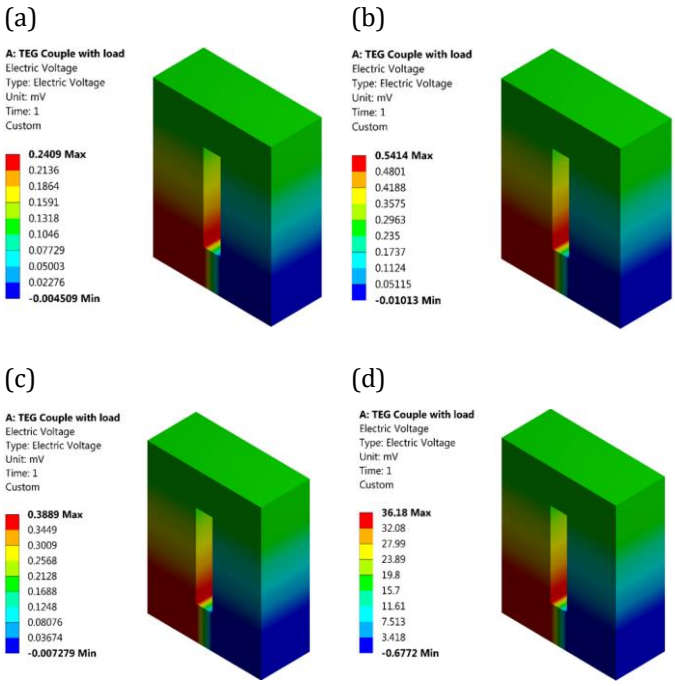

Fig. 16: Closed circuit voltage Contours of TEG couple at (a) hhs-10W/m²C and hcs- 10W/m²C, (b) hhs-10W/m²C and hcs-5000W/m²C, (c) hhs-5000W/m²C and hcs-10W/m²C and (d) hhs-5000W/m²C and hcs-5000W/m²C.

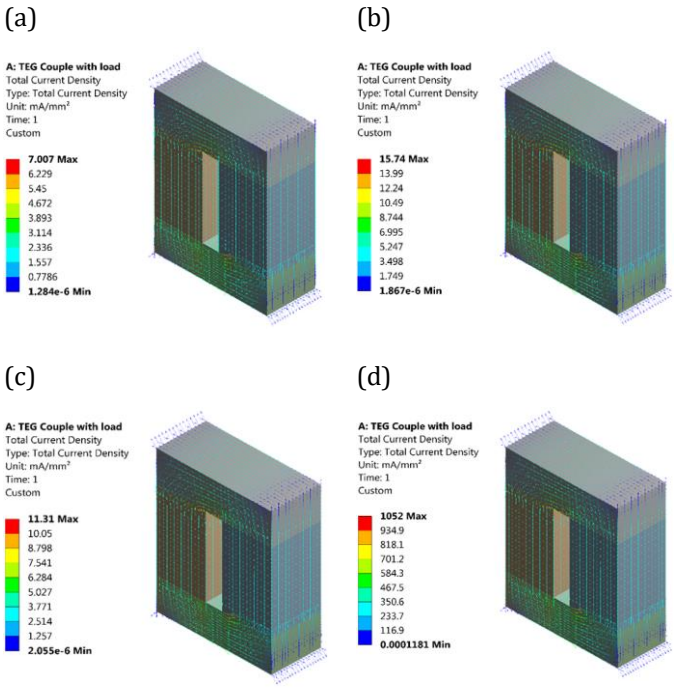

Fig. 17: Closed circuit Total current density vectors of TEG couple at (a) hhs-10W/m²C and hcs- 10W/m²C, (b) hhs-10W/m²C and hcs-5000W/m²C, (c) hhs-5000W/m²C and hcs-10W/m²C and (d) hhs-5000W/m²C and hcs-5000W/m²C.

3.3 Effect of heat source and heat sink temperature of TEG couple

The effect of heat source and heat sink temperature of TEG couple are studied through simulation considering the following input conditions. The hot side and cold side heat transfer coefficient considered are (hhs/hcs in W/m2C) 10/10,10/5000,5000/10 and 5000/5000 and the same square size of the p-type and n-type junction legs of 1.5 mm and the length of both the junction's legs are 2.5 mm. The thermal conductivity of TEG is assumed to be at 2.3 W/mC. Here, the influence of heat source and heat sink temperature on open circuit voltage and TEG power output is studied.

3.3.1 Effect of heat source and heat sink temperature of TEG couple for open circuit condition

The effect of heat source and heat sink temperature on and hot and cold side temperature of TEG couple is shown in Fig. 19 (a). The effect of heat source and heat sink temperature on open circuit voltage is shown in Fig. 19 (b). It can be observed that, for low heat source temperature, at different heat sink temperature, the drop in voltage and temperature difference is more when compared to higher heat source temperature for various heat sink temperature. The percentage difference in both voltage and temperature for set of heat source and heat sink temperature is more or less the same. It can be observed that the drop in the voltage and temperature difference is higher by increasing both heat sink temperature especially heat source temperature.

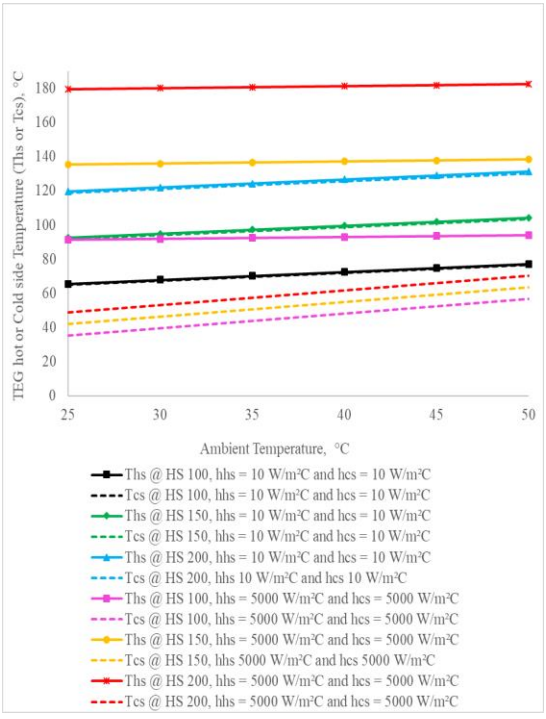

Fig. 19 (a): Effect of heat source and heat sink temperature on hot and cold side temperature of TEG couple.

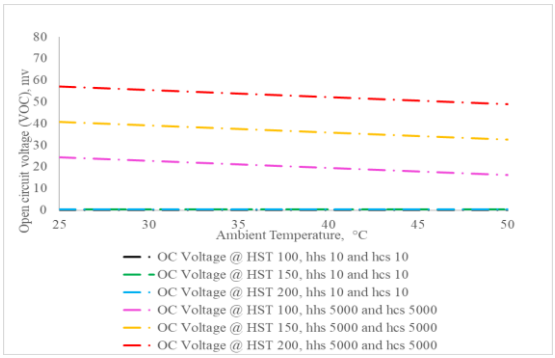

Fig. 19 (b): Effect of heat source and heat sink temperature on open circuit voltage of TEG couple.

3.3.2 Effect of heat source and heat sink temperature of TEG couple for closed circuit condition

The impact of TEG power output due to the effect of electrical load resistivity for typical set heat source and heat sink temperature is given by Fig. 20 to Fig. 23. It is observed that the power output of the TEG increases with the increase in heat source temperature and the power output is maximum at the matched load resistance. From the study, the matched load resistivity is found to be 0.00015 Ω-m. It is noted that the power output at heat source temperature of 200 °C is around 80 % higher than that at 100 °C when heat sink temperature is 25°C for a fixed heat transfer coefficient. Now, when heat sink temperature is increased to 50 °C, the percentage of power output is increased to 88% due to the influence of decrease in heat sink temperature with an increased source temperature. The percentage drop in power output at different heat sink temperature (Max 50 °C, Min 25 °C) is around 56 % at heat source temperature of 100 °C and the same is reduced to 14 % at the heat source temperature of 200 °C. This leads to the conclusion that, when the heat source temperature increases, there is no significant influence of heat sink temperature on TEG power output.

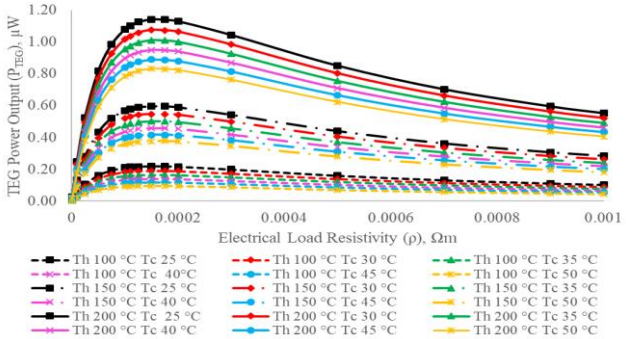

Fig. 20: Effect of TEG power output due to Electrical load resistivity for different heat source/heat sink temperature at hot/cold side heat transfer coefficient (10/10 W/m²C)

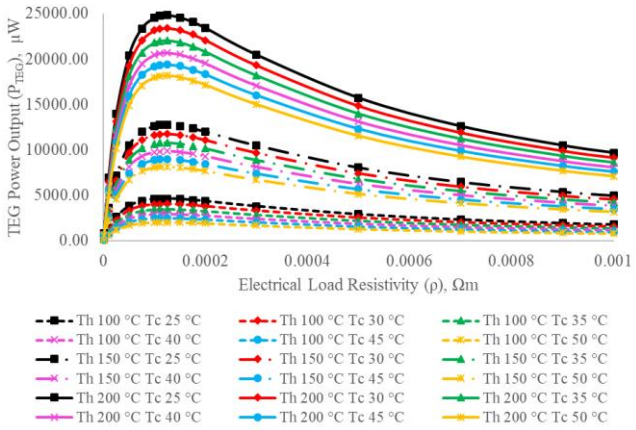

Fig. 21: Effect of TEG power output due to Electrical load resistivity for different heat source/heat sink temperature at hot/cold side heat transfer coefficient (5000/500 W/m²C)

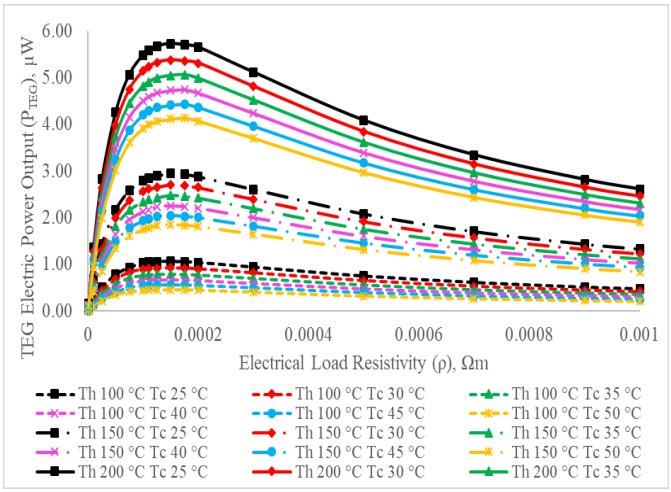

Fig. 22: Effect of TEG power output due to Electrical load resistivity for different heat source/heat sink temperature at hot/cold side heat transfer coefficient (10/5000 W/m²C)

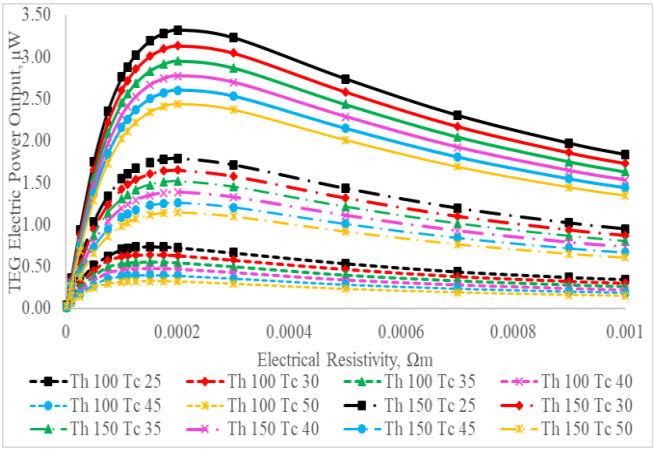

Fig. 23: Effect of TEG power output due to Electrical load resistivity for different heat source/heat sink temperature at hot/cold side heat transfer coefficient (5000/10 W/m²C)

Here, the influence of hot /cold side heat transfer coefficients impacting on voltage and power output are studied. And also, the impact of heat source/heat sink temperature on voltage and power output are studied. This concept is to be applied in thermal system configuration through literature study.

3. CONCLUSIONS

The importance of hot side and cold side heat transfer coefficients for TEG systems, in delivering the best performance is highlighted in this paper. Based on the simulation carried out by ANSYS 17®, the following results are concluded:

1. For a given low cold side heat transfer coefficient, increase in voltage and temperature difference is lesser when compared to higher hot side heat transfer coefficients for various cold side heat transfer coefficients.
2. For a set of hot side and cold side heat transfer coefficient, the percentage difference in voltage as well as for temperature will be almost the same.
3. As cold side heat transfer coefficient increases, the voltage and temperature difference will be higher.
4. The maximum power output is generated for each heat transfer coefficient with a highest individual value at matched load resistivity of 0.00015 Ωm.
5. When the cold side heat transfer coefficient is approximately 50 times higher than that of hot side heat transfer coefficient, the power output reaches saturation with increase in hot side heat transfer coefficient.
6. As heat source temperature and heat sink temperature is increased, the drop in the voltage and difference in temperature also increases.
7. When the heat source temperature increases, there is no significant impact on TEG power output by the heat sink temperature.

4. NOMENCLATURE

ZT = 'Figure of merit' of TEG
α = Seebeck coefficient of TEG couples in V/K
σ = Electrical conductivity of TEG couples in S/m
k = Thermal conductivity of TEG couples in W/mK.
hhs= TEG hot side Heat side heat transfer coefficient in W/m²C
hcs= TEG cold side Heat side heat transfer coefficient in W/m²C
Ths = Heat source temperature in °C
Tcs = Heat sink temperature in °C
Th = TEG hot side temperature in °C
Tc = TEG Cold side temperature in °C
ρ = Resistivity of Electric Load in Ωm
Vo = Ground on N-Junction bottom copper bar in mV
VOC = Open circuit Voltage in mV
PTEG = TEG Power Output in µW

REFERENCES

[1] Ohta H, Sugiura K, Koumoto K. Recent Progress in Oxide Thermoelectric Materials: p-Type Ca3Co4O9 and n-Type SrTiO3. Inorg Chem 2008; 47 (19); 8429–36.

[2] Rowe DM, Bhandari C. Modern thermoelectrics. Prentice Hall; 1983.

[3] Rowe DM, Min G. Evaluation of thermoelectric modules for power generation. J Power Sources 1998; 73 (2); 193–8.

[4] Riffat SB, Ma X. Thermoelectrics: a review of present and potential applications. Appl Therm Eng 2003; 23 (8);913–35.

[5] Hsiao YY, Chang WC, Chen SL. A mathematic model of thermoelectric module with applications on waste heat recovery from automobile engine. Energy 2010; 35(3); 1447–54.

[6] Hsu C-TY, Da-Jeng Ye, Ke-Jyun Yu, Ben. Renewable energy of waste heat recovery system for automobiles. J Renew Sustain Energy 2010; 2(1);013105.

[7] Ikoma KM, Furuya M, Kobayashi K, Komatsu M, Shinohara K. Thermoelectric generator for gasoline engine vehicles using Bi2Te3 modules. J Jpn Inst Met 1999; 63(11);1475–8 [Special Issue on Thermoelectric Energy Conversion Materials].

[8] Schlichting AD, Anton SR, Inman DJ. Motorcycle waste heat energy harvesting. In: The 15th International Symposium on: Smart Structures and Materials & Non-destructive Evaluation and Health Monitoring. 2008. International Society for Optics and Photonics.

[9] Takanose E, Tamakoshi H. The development of thermoelectric generator for passenger car. In: Proc 12th International Conference on Thermoelectrics. Yokohama, Japan, 1993.

[10] Brazdil M, Pospisil J. Thermoelectric power generation utilizing the waste heat from a biomass boiler. J Electron Mater 2013; 42(7); 2198–202.

[11] Moser WF, Günther Haslinger, Walter Hofbauer, Hermann. Small-scale pellet boiler with thermoelectric generator. In: Thermoelectrics, 2006. ICT'06. 25th International Conference on. IEEE, 2006.

[12] Kristiansen NR, Snyder GJ, Nielsen HK, Rosendahl L. Waste heat recovery from a marine waste incinerator using a thermoelectric generator. J Electron Mater 2012; 41 (6); 1024–9.

[13] Champier D, Bedecarrats JP, Rivaletto M, Strub F. Thermoelectric power generation from biomass cook stoves. Energy 2010; 35(2); 935–42.

[14] Moh'd A AN, Tashtoush BM, Khasawneh MA, Al-Keyyam I. A Hybrid Concentrated Solar Thermal Collector/Thermo-Electric Generation System. Energy. 2017 Jun 17.

[15] Dresselhaus MS, Chen G, Tang MY, Yang RG, Lee H, Wang DZ, et al. New directions for low-dimensional thermoelectric materials. Adv Mater 2007; 19 (8); 1043–53.

[16] Snyder GJ, Toberer ES. Complex thermoelectric materials. Nat Mater 2008; 7 (2); 105–14.

[17] Hsu KF, Loo S, Guo F, Chen W, Dyck JS, Uher C, et al. Cubic AgPbmSbTe2+m: bulk thermoelectric materials with high figure of merit. Science 2004; 303 (5659); 818–21.

[18] Poudel B, Hao Q, Ma Y, Lan Y, Minnich A, Yu B ,et al. High-thermoelectric performance of nanostructured bismuth antimony telluride bulk alloys. Science 2008; 320(5876); 634–8.

[19] Boukai AI, Bunimovich Y, Tahir-Kheli J, Yu J-K, Goddard Iii WA, Heath JR, et al. Silicon nanowires as efficient thermoelectric materials. Nature 2008; 451 (7175); 168–71.

[20] Hochbaum AI, Chen R, Delgado RD, Liang W, Garnett EC, Najarian M, et al. Enhanced thermoelectric performance of rough silicon nanowires. Nature 2008; 451(7175); 163–7.

[21] Zhao XB, JiXH, Zhang YH, Zhu TJ, Tu JP, Zhang XB, et al. Bismuth telluride nanotubes and the effects on the thermoelectric properties of nanotube-containing nanocomposites. Appl Phys Lett 2005; 86(6); 062111–3.

[22] Tang X, Xie W, Li H, Zhao W, Zhang Q, Niino M, et al. Preparation and thermoelectric transport properties of high-performance p-type Bi2Te3 with layered nanostructure. Appl Phys Lett 2007; 90(1); 012102–3.

[23] A Rezania, K Yazawa, LA Rosendahl, A Shakouri, Co-optimized design of micro channel heat exchanger and thermoelectric generators, International Journal of Thermal Science, 2013; 72; 73-81.

[24] Cheng-Ting Hsu, Gia-Yeh Huang, Hsu-Shen Chu, Ben Yu, Da-Jeng Yao, Experiments and simulations on low-temperature waste heat harvesting system by thermoelectric power generators, Applied Energy 2011; 88;1291–1297.

[25] Xiaolong Gou, Heng Xiao, Suwen Yang, Modeling, experimental study and optimization on low-temperature waste heat thermoelectric generator system, Applied Energy 2010; 87; 3131–3136.

[26] Xing Niu, Jianlin Yu, Shuzhong Wang, Experimental study on low-temperature waste heat thermoelectric generator, Journal of Power Sources 2009; 188; 621–626.

[27] Jianlin Yu, Hua Zhao, A numerical model for thermoelectric generator with the parallel-plate heat exchanger, Journal of Power Sources 2007; 172; 428–434.

[28] James W. Stevens, Optimal design of small DT thermoelectric generation systems, Energy Conversion and Management 2001; 42; 709-720.

[29] Nguyen Q. Nguyen, Kishore V. Pochiraju Behavior of thermoelectric generators exposed to transient heat Sources, Applied Thermal Engineering 2013; 51; 1-9.

[30] Lingen Chen, Jianzheng Gong, Fengrui Sun, ChihWu, Effect of heat transfer on the performance of thermoelectric generators, Int. J. Therm. Sci. 2002; 41; 95–99.

[31] Zhiqiang Niu, Hai Diao, Shuhai Yu, Kui Jiao, Qing Du, Gequn Shu, Investigation and design optimization of exhaust-based thermoelectric generator system for internal combustion engine, Energy Conversion and Management 2014; 85; 85–101.

[32] X. Liu, Y.D. Deng, K. Zhang, M. Xu, Y. Xu, C.Q. Su, Experiments and simulations on heat exchangers in thermoelectric generator for automotive application, Applied Thermal Engineering 2014; 71;364-370.

[33] Qing Du, Hai Diao, Zhiqiang Niu, Guobin Zhang, Gequn Shu, Kui Jiao , Effect of cooling design on the characteristics and performance of thermoelectric generator used for internal combustion engine, Energy Conversion and Management 2015;101; 9–18.

[34] Zhi-Gang Chen, Guang Han, Lei Yang, Lina Cheng, Jin Zou. Nanostructured thermoelectric materials: Current research and future challenge. Materials International 2012; 22(6); 535–549.

[35] M.C. Barma, M. Riaz, R. Saidur, B.D. Long, Estimation of thermoelectric power generation by recovering waste heat from Biomass fired thermal oil heater, Energy Conversion and Management 2015; 98;303–313.

[36] Xing Niu, Jianlin Yu, Shuzhong Wang, Experimental study on low-temperature waste heat thermoelectric generator, Journal of Power Sources 2009; 188; 621–626.

[37] Jianlin Yu, Hua Zhao, A numerical model for thermoelectric generator with the parallel-plate heat exchanger, Journal of Power Sources 2007; 172; 428–434.

[38] Zhiqiang Niu, Hai Diao, Shuhai Yu, Kui Jiao, Qing Du, Gequn Shu, Investigation and design optimization of exhaust-based thermoelectric generator system for internal combustion engine, Energy Conversion and Management 2014;85;85–101.